International Journal of Engineering & Technology, 7 (3.24) (2018) 32-39

International Journal of Engineering & Technology

Website: www.sciencepubco.com/index.php/IJET

Research paper

Micro Electro Discharge Machining of Nonconductive Ceramic: The Issue of Spalling

Mohammad Yeakub Ali*, Abdus Sabur, Md. Abdul Maleque

Department of Manufacturing and Materials Engineering
International Islamic University Malaysia
PO Box 10, 50728 Kuala Lumpur, Malaysia
**Corresponding author E-mail : mmyali@iium.edu.my*

Abstract

Nonconductive ceramic materials are used in many engineering applications such as car brake, turbine blade, and hip-bone replacement because of its high dimensional accuracy, corrosion and wear resistant, and biocompatibility. These materials are usually processed with diamond grinding and limited laser applications such as cutting, drilling and scribing. Specific shapes and profiles are still difficult and costly to machine using these processes. Electrical discharge machining (EDM), extensively used for various shapes and profiles on conductive materials having minimum electrical conductivity of 0.10 S.cm-1. It is not directly applicable on nonconductive ceramic materials due to its very low electrical conductivity (<10-10 S.cm-1). However, recently EDM is used on nonconductive materials with the aid of assisting electrode to initiate the spark between conductive tool electrode and nonconductive workpiece. The available material removal models of EDM are based on single spark erosion with uniform melting and vaporization of workpiece materials. However, in EDM of nonconductive ceramics, material removal is not uniform because of random spalling due to alternating thermal stress. In addition, it is difficult to create single spark erosion on a nonconductive ceramic workpiece as initial sparks are occurred between tool electrode and assisting electrode attached to workpiece. This paper presents the empirical factor for the estimation of spalling along with melting and vaporization through experimental study. Model of material removal rate as a function of capacitance and voltage are developed in micromachining of nonconductive zirconium oxide (ZrO_2) using (R-C) pulse type micro-EDM. The single spark erosion volume is derived from the fundamental principle of melting and vaporization. An empirical correction factor is introduced to compensate random spalling and multi-spark erosion effect.

Keywords: *Assisting electrode; Carbonic dielectric fluid; Material removal; Micro-EDM; Nonconductive ceramic; Pyrolytic carbon; Spalling.*

1. Introduction

Nonconductive ceramic materials have been used for a variety of biomedical and implant devices [Chevalier and Gremillard, 2009; Bonny et al., 2009]. But these materials are difficult to process by conventional micro-machining techniques due to high hardness and brittleness [Hosel et al, 2011]. Micro-electro discharge machining (micro-EDM), a noncontact process, is a suitable technique for microstructuring in which a series of electrical sparks or discharges occur rapidly in a short span of time between tool electrode and workpiece. The electrical energy is converted into thermal energy instantaneously during micro-EDM which causes the melting and evaporation of the material. The material to be machined by micro-EDM requires a minimal electrical conductivity of 0.1 Scm-1 [Hosel et al., 2011; Hosel et al., 2011a; Patel et al., 2010]. Most of the advanced ceramics such as ZrO_2, Al_2O_3, Si_3N_4 are electrically nonconductive, therefore, EDM cannot be used directly [Mohri et al., 1996; Banu, Ali and Rahman, 2014]. An advanced technique is introduced to use EDM for machining the nonconductive ceramic materials in which an assisting electrode (AE) of electrically conductive material is applied on the surface of the workpiece. The sparks initially occur between the tool electrode and the AE. After finishing the AE, a layer of pyrolytic carbon (PyC) is deposited on the workpiece surface disassociating the carbonic dielectric in absence of oxygen and at a temperature of 1000-20000C. In experimental investigations it is observed that during the R-C pulse micro-EDM of nonconductive ceramics, pulse-off time is longer than that in conductive materials and effect of alternating thermal stress resulting spalling in addition to melting and evaporation [Chen et al., 2010; Sabur et al., 2013; Schubert et al., 2011; Schubert et al., 2015]. Sometimes, spalling becomes dominant over other removal mechanisms. It is observed that in rough EDM of the nonconductive ceramics, materials are mostly removed by spalling whereas in finish EDM the removal occurs mainly due to melting and evaporation [Liu et al., 2008].

Most of the available theoretical models for materials removal are established for conductive materials based on the single spark analysis where many issues such as ignition delays, frequency of sparks, flushing are assumed negligible [Izquierdo et al., 2009; Salonitis et al., 2009]. In micro-EDM of nonconductive ceramics, sparks occur initially on the conductive AE layer and workpiece material is removed after the removal of AE material. As a result, the effect of single spark on the ceramic workpiece is difficult to investigate. Therefore, modelling of MRR considering the multi-sparks is essential. Spalling is a random phenomenon and difficult to incorporate in the thermal models with a single pulse discharge [Liu et al., 2009]. Therefore, it is difficult to estimate the MRR of nonconductive ceramic workpiece using conventional approach. The theoretical model established for single spark is needed to be adjusted. This adjustment can be done by a correction factor to

Copyright © 2018 Authors. This is an open access article distributed under the Creative Commons Attribution License, which permits unrestricted use, distribution, and reproduction in any medium, provided the original work is properly cited.

encounter the spalling and multi-spark effect in micro-EDM of nonconductive ceramic materials. This paper aims to develop a model of MRR using the relevant fundamental electro-thermal theories with experimental correction measure for R-C pulse micro-EDM of nonconductive ZrO_2 ceramic.

2. MRR for Conductive Materials

Assumptions:

i) The workpiece and tool materials are homogeneous in nature.
ii) The thermo-physical properties of the workpiece material remain constant during the machining process [Wong et al., 2003].
iii) A fraction of the total spark energy is absorbed into the workpiece by conduction and rest of the energy is dissipated to the surroundings by convection and radiation [Zahiruddin and Kunieda, 2012].
iv) The entire material is removed from the cavity after each discharge [Kiran et al., 2007] and debris is not re-solidified inside or around the cavity.
v) The capacitor has no initial voltage and it is charged from a constant voltage source.
vi) Ignition delay time is negligible compared to total charging and discharging time.

2.1. Formulation of MRR

R-C pulse micro-EDM circuit has mainly two parts. The charging part is connected to a high resistor in series. The discharging part has no resistor or is connected to a very low resistor. The energy stored in the capacitor during the charging period is released through the gap. The energy discharged in a single spark is given by Eqn (1).

$$E = \frac{1}{2} CV^2 \tag{1}$$

In R-C pulse circuit, the product of RC is known as 'time constant' and it has been proved that about 99% of capacitor charging and discharging occurs within five time constant. Assuming R1 and R2 are the resistance in charging and discharging circuit respectively, then the cycle time is 5(R1 + R2)C. Total number of sparks per second (Ns), is the reciprocal of total time required for single spark as expressed by Eqn (2). The total number of sparks in unit time is the function of capacitance and resistances. Therefore, Ns can be increased or decreased by changing either the capacitance or resistances or both in a R-C pulse micro-EDM circuit.

$$N_s = \frac{1}{5(R_1 + R_2)C} \tag{2}$$

It is observed that each cycle has three stages. The first stage is called charging or pulse-off time when capacitor receives charges from the electric source and the capacitor voltage rises to its full capacity while its current decreases to zero. The second stage is referred to ignition delay where dielectric breakdown occurs under the electromagnetic field and the resistance between tool and workpiece decreases to zero. The third is called discharging or pulse-on time stage. In this stage there is virtually no resistance between the tool and workpiece and spark occurs with high current. The capacitance voltage decreases to zero. In this study, ignition delay is assumed negligible compared to the total charging and discharging time. In addition, the charging and discharging time depends on the amount of capacitance and resistances in the circuit. To make a very quick discharge, the discharge circuit is kept resistance-free. However, the discharge circuit experiences a small resistance from dielectric fluid and the machine system [Alexander, et al., 2007].

The single spark energy of an R-C micro-EDM circuit as expressed by Eqn (1) is not utilized completely for material removal of the workpiece. Only a fraction of the spark energy causes melting and vaporization of the material and creates a micro-crater. The remaining energy supplied into the gap is lost to the surroundings [Zahiruddin and Kunieda, 2012]. Thus energy is required for melting and vaporizing of unit kilogram of workpiece material, Hm and Hv respectively are expressed by Eqn (3) and (4).

$$H_m = c_p(T_m - T_i) + L_m \tag{3}$$

$$H_v = c_p(T_b - T_i) + L_m + L_v \tag{4}$$

Assuming, k1 fraction of E is used to vaporize and k2 fraction of E is used to melt the material only. Thus, the volume of material removed per spark can be found using Eqn (5).

$$V_r = \frac{CV^2}{2\rho}\left[\frac{k_1}{H_v} + \frac{k_2}{H_m}\right] \tag{5}$$

According to Eqn (5), the crater volume is the function of capacitance, voltage and volumetric heat of vaporization and melting. Thus, material removal is controlled by both the electrical parameters and thermal properties of the work material in R-C pulse micro-EDM. The material removal rate (MRR) is defined as the volume of material removed per unit time and is expressed by Eqn (6).

$$MRR = \frac{N_s}{2\rho}\left[\frac{k_1}{H_v} + \frac{k_2}{H_m}\right] CV^2 \tag{6}$$

This is the expression of MRR based on single spark erosion due to melting and vaporization in R-C pulse micro-EDM which shows that the electrical parameters, number of sparks per unit time and thermal properties of the material directly control the erosion rate. In this formulation 100% sparks are considered effective for material removal. However, in practice, only 30-50% of total sparks are found to be effectively used in material removal in micro-EDM of conductive materials [Liao et al., 2008; Schubert et al., 2013]. In this research, nine experiments were conducted with various combination of capacitance (105, 104 pF) and voltage (100, 90, 80 V) on cooper workpiece using die-sinking micro-EDM machine (DT-110, Mikrotools Inc., Singapore). A schematic diagram of the experimental setup for micro-EDM of nonconductive ceramics with AE is shown in Figure 1. One of the machined cavity, as inspected by scanning electron microscope (SEM) is shown in Figure 2. When comparing the theoretical (Eqn 6) and experimental MRR, it was found that on the average only 46% of total energy is effective for material removal. So, considering the practical implication, Eqn (6) is to be re-written as Eqn (7) for multi-spark erosion.

In multi-spark machining, charging and discharging do not always follow the estimated time constant [Izquierdo et al., 2009], and ineffective pulses such as arching and short circuit are frequent [Aligiri et al., 2010]. All these conditions reduce the effective number of pulses per second, which in turn reduces MRR. The SEM investigation (Figure 2) revealed that copper micro-crater is having a clear and identical geometric pattern with minimum inaccuracy because of uniform removal of material by melting and vaporization. This result is agreeable with similar study of micro-EDM of conductive materials [Zahiruddin and Kunieda, 2012].

$$MRR = \frac{N_s}{4\rho}\left[\frac{k_1}{H_v} + \frac{k_2}{H_m}\right] CV^2 \tag{7}$$

$$MRR_C = \varepsilon \frac{N_s}{4\rho}\left[\frac{k_1}{H_v}+\frac{k_2}{H_m}\right]CV^2 \quad (8)$$

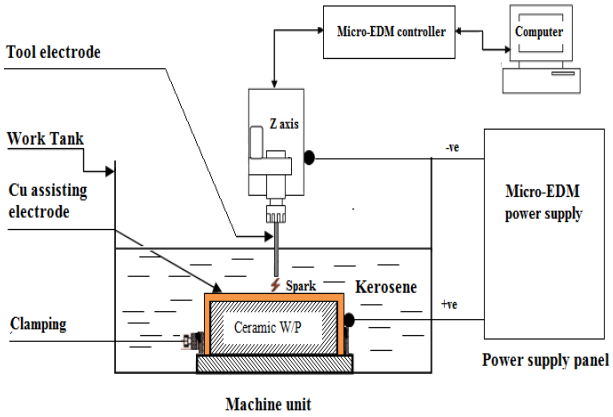


Fig. 1: Schematic diagram of micro-EDM setup

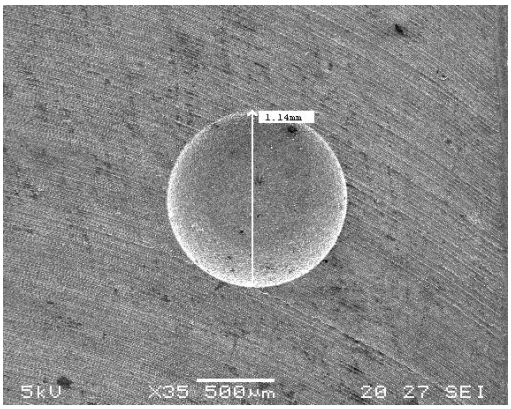


Fig. 2: SEM micrograph of microcavity on copper workpiece (Machining parameters: C = 105 pF, V = 100 V)

2.2. MRR for Micro-EDM of Nonconductive Ceramic

In micro-EDM of nonconductive ceramics, material removal is controlled by spalling (flake by flake). Therefore, Eqn (7) is not directly applicable for nonconductive ceramic materials and modification is needed. In this study, a multiplying factor is proposed as a corrective measure. Hence, the material removal rate for nonconductive ceramics, MRRC, is expressed by Eqn (8). The correction factor ε is to encounter the spalling effect. This effect can be encountered by analytical and or empirical approach.
However, due to the random nature and size of the spalled materials, analytical approach could be a tedious task. In this study, the correction factor ε is determined empirically as a function of C and V, the energy parameters that caused thermal stress on nonconductive ceramic workpiece.

2.2.1 Experiments to Estimate ε

To get the correction factor ε, micro-EDM experiments have been conducted. Experiments were conducted using a die-sinking micro-EDM machine (DT-110) to investigate the levels of parameters and their combination that are effective for machining. The preliminary experimental conditions of this study for identification of parameters and levels for effective micro-EDM of ZrO_2 are listed in Table 1.

Table 1: Preliminary experimental conditions for effectiveness of micro-EDM of ZrO_2

Conditions/ properties	Description/Value
Workpiece	ZrO_2 (purity 92%)
Tool electrode	Copper (ϕ 1 mm)
Tool electrode polarity	+ve, -ve
Assisting electrode	Adhesive copper foil
AE thickness (µm)	60
Dielectric fluid	Kerosene
Capacitance, *C* (pF)	10^5, 10^4, 10^3, 10^2, 10^1, 470
Voltage, *V* (V)	110, 100, 90, 80
Tool electrode speed, *n* (rpm)	250, 275, 300, 350
Feed rate, *f* (µm/s)	1, 2
Resistance in charging circuit, R_1 (Ω)	1000 (fixed)
Resistance in discharging circuit, R_2 (Ω)	1 (assumed)

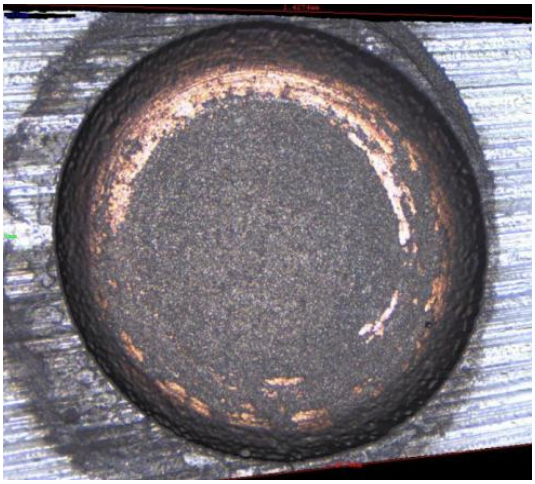


Fig. 3: Micro-hole on ZrO_2 workpiece machined by micro-EDM using adhesive Cu foil as AE and Cu tool electrode with –ve polarity (Machining parameter: 10 pF capacitance and 80 V voltage)

A workpiece coated with adhesive copper (Cu) foil as AE was machined using 1 mm diameter Cu electrode and kerosene dielectric. Spark was initiated between the tool electrode and the Cu layer. After the removal of Cu foil, a new conductive layer of pyrolytic carbon (PyC) was produced instantaneously on the machined surface by dissociating the carbon chain of kerosene. Melted conductive particles of Cu were mixed with PyC, which also enhanced the conductivity. The results (yes/no) of the preliminary experimental study for identification of parameters are listed in Table 2. It was observed that higher capacitances (>103 pF) are not effective and not capable of producing a continuous PyC layer on the workpiece. It was also observed that effective parameters are capacitance of 101-103 pF and voltage of 80-100 V or capacitance of 10-470 pF and voltage of 80 - 110 V. The copper tool electrode with positive polarity was also not effective in micro-EDM of ZrO_2. Finally, experiments were conducted according to the Taguchi design of experiments for determination of ε using the parameters selected based on preliminary experiments. The selected variable and fixed parameters for Taguchi experimental design are listed in Table 3. There are nine experiments which were conducted using DT 110 with the machine setup shown in Figure 1. One of the machined micro-holes is shown in Figure 3. After each machining, the experimental MRR was calculated. The theoretical MRR was calculated using Eqn (7). The experimental material removal rate (MRRex) was calculated by Eqn (9) where d = average radius of the hole, h = average depth of the hole, and tex = the total machining time. Correction factor (εi) was calculated as the ratio of experimental MRRex (Eqn 9) to theoretical MRR (Eqn 7) for each run using Eqn (10).

$$MRR_{ex} = \frac{\pi d^2 h}{4 t_{ex}} \quad (9)$$

$$\varepsilon_i = \frac{MRR_{ex}}{MRR} \quad (10)$$

$$\varepsilon = [-0.061 + 0.00013 \times C + 0.0031 \times V]^2 \quad (11)$$

$$MRR_c = \frac{N_s}{4\rho}\left[-0.061 + 0.00013C + 0.0031V\right]^2 \left[\frac{k_1}{H_v} + \frac{k_2}{H_m}\right] CV^2 \quad (12)$$

Table 2: *Preliminary experimental results of micro-EDM of ZrO_2*

No	Capacitance C (pF)	Voltage V (V)	Speed n (rpm)	Feed rate f (µm/s)	Electrode polarity	Significant machining (Yes/ No)
1	10^5, 10^4	80-100	250-350	1-2	-, +	No
2	10, 100, 220, 330, 470	80-110	250-350	1-2	+	No
3	10^3	110	250-350	1-2	-, +	No
4	10^3	80-100	250-350	1-2	-	Yes
5	10, 100, 220, 330, 470	80-110	250-350	1-2	-	Yes

Table 3: *Variable and fixed parameter for micro-EDM of ZrO_2*

Condition Variables	Value Level		
	I	II	III
Capacitance, *C* (pF)	10	100	1000
Voltage, *V* (V)	80	90	100
Speed, *n* (rpm)	250	300	350
Feed rate, *f* (µm)	1.2	1.6	2
Fixed Parameter			
Tool electrode	Cu, ϕ 1 mm		
Tool polarity	-ve		
Assisting electrode, thickness (µm)	Adhesive Cu foil, 60		
Dielectric fluid, flushing type	Kerosene, non-flushing		
Threshold (%)	27		
Machining depth (µm)	200		
Resistance in charging circuit (Ω)	1000		
Resistance in discharging circuit (Ω)	1		

Each of the nine test run was repeated three times to avoid any biasness. Then, the mean values of the three machining results were used as the output for each set of parameters. The calculated correction factor values are shown in Table 4. To derive the correction factor (ε) in terms of process parameters, experimental data was analysed using ANOVA as shown in Table 5. The effect of speed and feed rate were observed to be insignificant towards ε. Therefore, the final eqn of ε in terms of actual factors (with the transformation of square root) is expressed by Eqn (11) where = capacitance (pF), and V = voltage (V). Substituting the value of ε in Eqn (8), the theoretical MRR in micro-EDM of ZrO_2 with a correction factor can be expressed by following Eqn (12) where Ns = number of sparks per second, C = capacitance of the capacitor, V = gap voltage, k1 = fraction of energy E used to vaporize the material, k2 = fraction of energy E is used to melt the material, ρ = density of the work material, Hv = heat of vaporization, Hm = heat of melting. Eqn (12) is applicable in micro-EDM of ZrO_2 for the capacitance range of 101 -103 pF and the voltage range of 80-100 V. The value of k1 and k2 varies according to workpiece properties such as thermal conductivity, hardness, diffusivity and machining condition [Zahiruddin and Kunieda, 2012; Dhanik and Joshi, 2005].

Table 4: *L9 orthogonal array for micro-EDM of ZrO_2 for ε*

	Parameters				Response
No.	A:Capacitance C (pF)	B: Voltage V (V)	C: Speed n (rpm)	D: Feed rate f (µm/s)	Average correction factor, (εi)
1	1000	100	300	1.2	0.064523
2	1000	90	250	2	0.058079
3	1000	80	350	1.6	0.051052
4	100	100	250	1.6	0.047500
5	100	90	350	1.2	0.030734
6	100	80	300	2	0.020619
7	10	100	350	2	0.023004
8	10	90	300	1.6	0.017785
9	10	80	250	1.2	0.015451

Table 5: *Analysis of variance for ε*

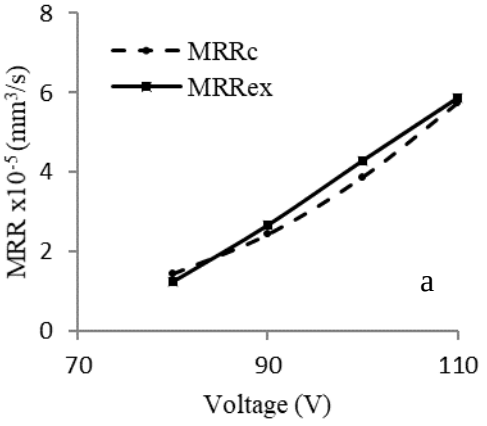
Source	Sum of squares	DF	Mean square	F value	Prob > F
Model	0.017383	2	0.008691	20.47264	0.0021
A	0.014575	1	0.014575	34.33232	0.0011
B	0.002807	1	0.002807	6.612964	0.0422
Residual	0.002547	6	0.000425		
Cor Total	0.01993	8			
Std. Dev.	0.020604		R-Squared	0.872192	
Mean	0.185238		Adj R-Squared	0.829589	
C.V.	11.12319		Pred R-Squared	0.727925	
PRESS	0.005422		Adeq Precision	11.12928	

2.2.2 Model Validation

The model (Eqn 12) was verified by experimental study with machining parameters as shown in Table 6. For each of the capacitance, experiments were conducted for three different voltages of 90, 95, and 100 V. Other parameters are kept constant as in Table 6. MRRC, the theoretical values have been obtained by using Eqn (12) and experimental values were calculated after micro-EDM of ZrO_2. Figure 4 shows the comparison between the theoretical and experimental MRR at different parameter conditions. It is observed that both the theoretical and experimental MRR are coherent at capacitance of 100 pF, 220 pF and 330 pF (Figure 4a-c) because of higher numbers of effective sparks produced.

But, at higher capacitance and higher voltage, deviation of the MRRc with MRRex is noticeable (Figure 4d). It can be said that at higher energy levels, stable PyC were not formed and practically the material removal was decreased. Therefore, a higher deviation between MRRc and MRRex was observed. The average differences has been found to be around 10%. In previous studies, it was stated that the material removal in EDM of ceramic is mainly by spalling which is difficult to encounter [Hosel et al., 2011; Ji et al., 2012; Trueman and Huddleston, 2000]. However, in this study the spalling effect is encountered by empirical study.

The machined surface texture of ZrO_2, as shown in Figure 5, reveals that the crater of nonconductive ceramics contains many irregular globules as an evident of spalling. The ZrO_2 workpiece has also been investigated by EDX before and after micro EDM machining and the spectrum shown in Figure 6. In comparison of Figure 6a and Figure 6b, a significant carbon content is evident after micro EDM with carbonic dielectric fluid. This carbon percentage is used to make the instantaneous conductive layer on the nonconductive ceramic workpiece which eventually help to continue electro discharge machining.



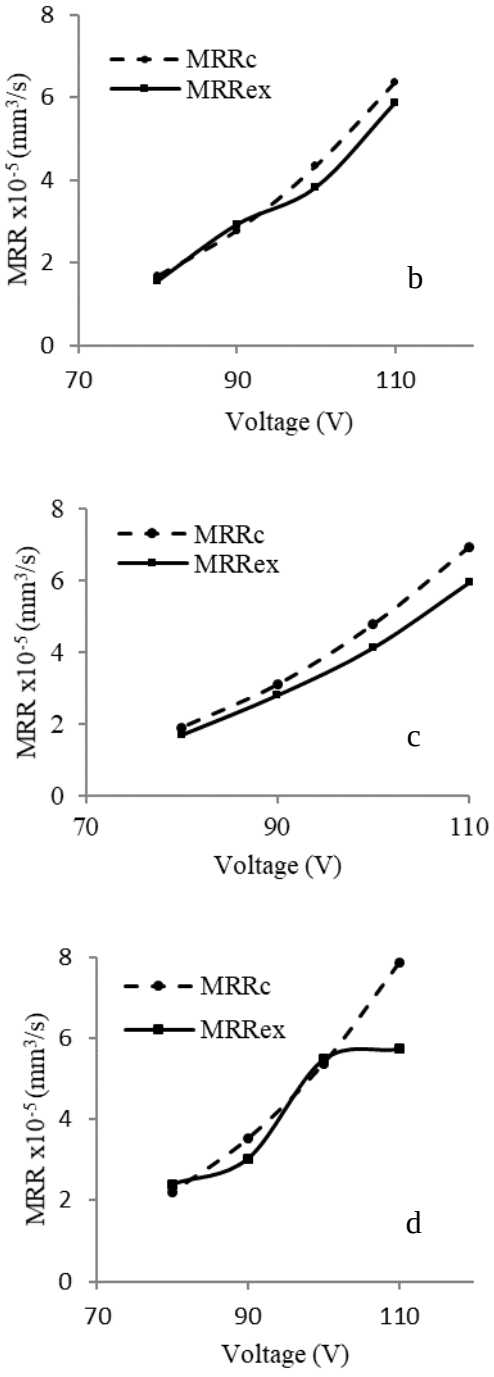


Fig. 4: Theoretical and experimental MRR in micro-EDM of ZrO_2 vs. voltage at capacitance (a) 100 pF, (b) 220 pF, (c) 330 pF, and (d) 470 pF

Table 6: *Experimental conditions for validation of models*

Variables	Level		
	I	II	III
Capacitance, C (pF)	100	220	470
Voltage, V (V)	90	95	100
Fixed Parameter			
Speed, *n* (rpm)	300		
Feed rate, *f* (µm)	0.2		
Tool electrode, diameter (mm), polarity	Cu, ϕ 1 mm, -ve		
Assisting electrode, thickness (µm)	Adhesive Cu foil, 60		
Dielectric fluid, flushing type	Kerosene, non-flushing		
Threshold (%)	27		

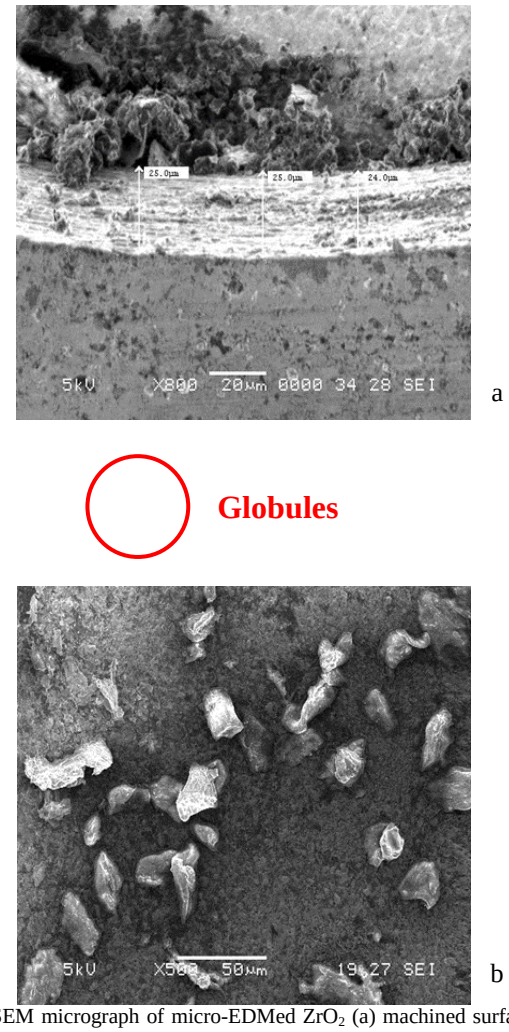


Fig. 5: SEM micrograph of micro-EDMed ZrO_2 (a) machined surface (b) zoom-in view of window A on the machined surface (Machining parameters: C = 100 pF, V = 90 V)

3. Results and Discussions

During the EDM of nonconductive ceramic machining, rate of effective spark becomes much lower than that in conductive materials. This circumstance requires the introduction of a correction factor based on experimental studies of percentage of effective sparks and cycle characteristics in micro-EDM of ZrO_2. During machining of nonconductive ZrO_2, experimental investigation using oscilloscope (MSO 4104, Tektronix, USA) and voltage probe (P6139A, Tektronix, China) has been performed where different type of pulses are observed as shown in Figure 7. Regular discharges are identified in initial stage when the Cu AE layer was machined (Figure 7a). The capacitance was charged about 99% of the machine setup voltage and reached below 2% after discharges. After charging, the energy is released by spark without any delay. Similar trend remained at the beginning of ceramic machining. As the machining progressed, pulse shapes began to change and voltage remained at peak for long period than the normal discharge (Figure 7b). These long-hold-peak voltage pulses take longer pulse-off time that reduces MRR eventually. There are some discharges, known as delayed discharges that have occurred before the capacitor has been fully charged. Shape of the delayed discharges is similar to normal discharges with lower peak current and lower duration.

Another voltage shape is observed in micro-EDM of ZrO_2 at deeper holes. The sparks occurred after the capacitor reached its peak voltage and charges are not fully released. Capacitor started charging at higher voltage instead of returning from peak to zero (Figure 7c). These are short sparks. Charging at higher than set up

voltage and incomplete discharge cause low energy supply for material removal. The delayed discharge, arching, short circuit, short sparks are considered ineffective and the total energy supplied by sparks per unit time is considerably reduced.

In addition, the continuous formation of conductive PyC layer on the workpiece surface and removal of this layer consume a certain amount of energy. In this study, formation energy to produce pyrolytic carbon (PyC) during micro-EDM is considered negligible. Therefore, different types of ineffective pulses and formation of PyC reduce the total energy per unit time. As a result, experimental MRR becomes very low compared to theoretical MRR to be in micro-EDM of ceramic materials.

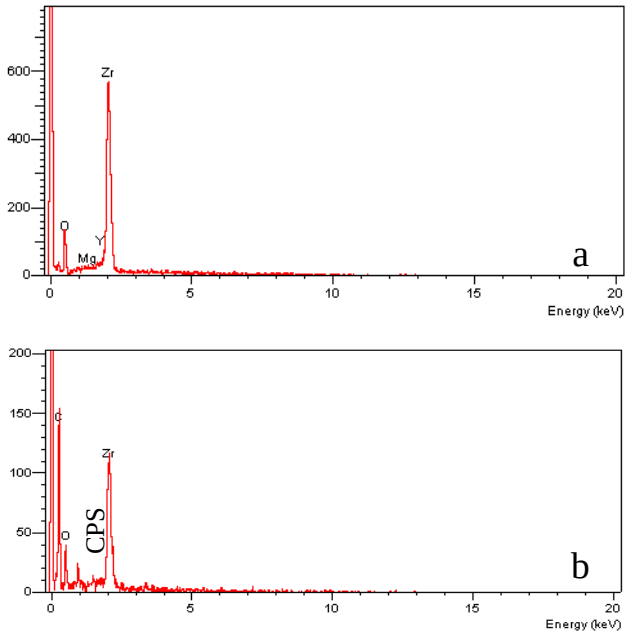


Fig. 6: EDX spectrogram of ZrO_2 workpiece (a) before, and (b) after machining using micro-EDM

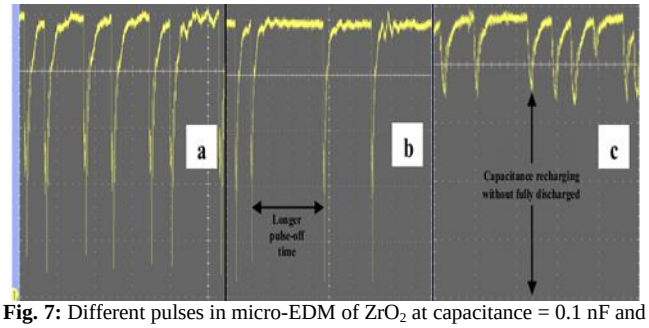


Fig. 7: Different pulses in micro-EDM of ZrO_2 at capacitance = 0.1 nF and Voltage = 100V (a) normal discharges, (b) ceramic discharges with long-hold period at peak, (c) charging and discharging at higher values than set up voltage

Table 7: *Machining conditions for micro-EDM of ZrO_2*

Parameters (unit)	Conditions
Workpiece, purity (%)	ZrO_2, 92
Tool electrode, diameter (µm), polarity	Cu, 900, -ve
Assisting electrode, thickness (µm)	Adhesive Cu foil, 60
Dielectric, flushing	Kerosene, non-flushing
Capacitance (pF), voltage (V)	100, 80; 100, 95; 220, 98
Rotational speed, *n* (rpm)	250
Feed rate, *f* (µm)	0.10
Workpiece, purity (%)	ZrO_2, 92
Tool electrode, dia. (µm), polarity	Cu, 900, -ve
Assisting electrode, thickness (µm)	Adhesive Cu foil, 60
Dielectric, flushing	Kerosene, non-flushing
Capacitance (pF), voltage (V)	100, 80; 100, 95; 220, 98

Table 8: *Comparison of estimated and measured MRR*

	C (pF)	V (V)	Eqn. 12 $MRR_C \times 10^{-5}$ (mm^3/s)	Measured $MRR \times 10^{-5}$ (mm^3/s)	% error
1	100	80	2.0	1.80	10.00
2	100	95	3.0	2.72	9.30
3	220	98	4.0	3.71	7.25
4			Average		8.86

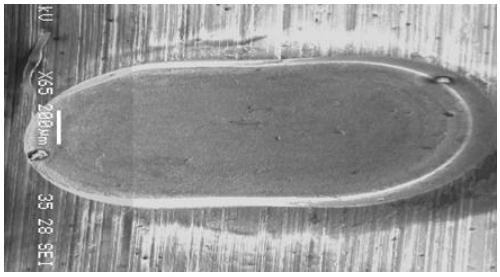


Fig. 8: SEM micrograph of micro-channel on ZrO_2 by micro-EDM with C=100 pF and V=80 V

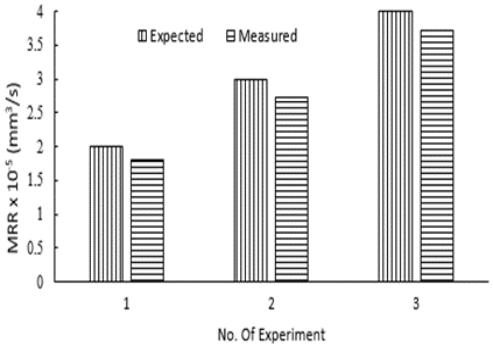


Fig. 9: Comparison of expected to experimental MRRc in micro-EDM of micro-channel on ZrO_2

4. Application of Model

The findings of this theoretical and experimental study are applied in machining of a microcavity on ZrO_2 as shown in Figure 8. Solving Eqn (12), values of capacitance and voltages have been selected for the expected MRRC. Using these parameters, 200 µm deep microcavity was machined with micro-EDM (DT-110). The machining conditions are given in Table 7. Adhesive copper foil AE, ϕ 900 µm Cu tool electrode, and kerosene dielectric fluid were used in this experiment. The spark occurred initially between the copper assisting electrode and the tool electrode. After removal of the adhesive foil, a conductive carbonic layer was deposited on the machined surface which acted as an assisting electrode to continue spark generation. Three runs of experiment for each parameter combinations are conducted and the average of these results is taken. Microcavity was investigated using SEM. The machining parameters, predicted MRR and experimental MRR are listed in Table 8. A pictorial comparison of expected to experimental values of MRR is shown in Figure 9. As the average error is found to be 8.8 %, the model is considered validated as 20% error is acceptable by the researchers [Abbas et al., 2007].

SEM investigation also showed that the microcavity lacks in geometrical integrity. The diameter of the tool electrode reduces due to wear, subsequently; the width of the channel also reduces. To minimize the effect of tool wear, the tool electrode should be dressed or new tools should be used for machining microcavities with accurate dimensions.

5. Conclusion

In this study, MRR model is developed for R-C pulse micro-EDM based on fundamental electro-thermal theories to establish the

functional relationship of MRR with materials properties and micro EDM process parameters capacitance and voltage. Although the model is found to be valid for conductive materials, it needs a correction or adjustment factor when applied on nonconductive ceramic materials mainly because of ineffective sparks and spalling issues. As such a correction factor (ε) is introduced and its significance was identified through Taguchi design based experimental study of MRR in micro-EDM of nonconductive ceramics.

In this study Cu tool electrode, adhesive Cu foil as AE, and kerosene dielectric fluid are used to drill micro-holes on ZrO_2 ceramic workpiece. From this analytical and experimental study, the following specific conclusions can be made:

i) It is found that the experimental MRR is very low compared to the theoretical values due to the longer pulse-off time, delayed discharge, short circuit, arching, and immature discharges in micro-EDM of nonconductive ceramics. The formation energy of PyC is also not quantified. Therefore, in addition to spalling effect, the correction factor (ε) also includes the energy of formation and dissociation for PyC and the effect of unwanted pulses.
ii) In micro-EDM of nonconductive ZrO_2 ceramic, capacitance is found to be the most significant parameter for creation of conductive PyC layer. No significant material removal occurred if the capacitance is higher than 1 nF. The voltage in the range of 80-100 V is found to be more effective for MRR.
iii) Micro-cavities have been created on ZrO_2 with selected parameters for the expected MRRC values as one of the applications of micro-EDM models. It was shown that the MRRC in micro-EDM of ZrO_2 were found to be in agreement with the calculated expected values by an average error of 8.86 %.
iv) Industries will be able to use this model and select parameters without further experiments, which in turn will increase efficiency and reduce cost of production in microstructuring of ZrO_2 ceramic. Using the technique followed in this study, necessary correction factors for micro-EDM of other nonconductive ceramics such as Al_2O_3, Si2N4 and SiC can be formulated. Further study is needed to investigate the effect of energy on the formation of the PyC layer at different parameter levels.
v) Previous studies of EDM for non-conductive ceramics concentrated on process development where spalling issues were highlighted [Chen et al., 2010; Liu et al., 2008; Liu et al., 2009] but no mathematical relationship for the estimation of spalling has been reported. As spalling is a random phenomenon, this study successfully developed mathematical relationship based on fundamental and experimental approach for the estimation of spalling effect.

Acknowledgement

The authors would like to thank the Ministry of Science, Technology and Innovation (MOSTI), Malaysia for financial support under Science Fund Research Project 03-01-08-SF0135.

Nomenclature

Boiling temperature, T_b (°C)
Capacitance, C (F)
Density, ρ (Kg/mm^3)
Single spark energy discharge, E (J)
Feed rate, f (µm/s)
Fraction of E consumed by melting, k_1
Fraction of E consumed by vaporization, k_2
Heat of melting, H_m (J/Kg)
Heat of vaporization, H_v (J/Kg)
Latent heat of melting, L_m (J/Kg)
Latent heat of vaporization, L_v (J/Kg)
Melting temperature, T_m (°C)
No. of sparks per second, N_s
Resistance in charging circuit, R_1 (Ω)
Resistance in discharging circuit, R_2 (Ω)
Rotational speed of tool, n (rpm)
Specific heat, C_p (J/Kg^{0}C)
Voltage, V (V)

References

[1] Chevalier, J., & Gremillard, L. (2009). Ceramics for medical applications: a picture for the next 20 years. *Journal of the European Ceramic Society*, 29 (7), 1245-1255.
[2] Bonny, K., De Baets, P., Vleugels, J., Salehi, A., Van der Biest, O., Lauwers, B., & Liu, W. (2009). EDM machinability and fractional behavior of ZrO_2-WC composites. *International Journal of Advanced Manufacturing Technology*, 41 (11-12), 1085-1093.
[3] Hosel, T., Muller, C., & Reinecke, H. (2011). Spark erosive structuring of electrically nonconductive zirconia with an assisting electrode. *CIRP Journal of Manufacturing Science and Technology*, 4 (4), 357-361.
[4] Hosel, T., Cvancara, P., Ganz, T., Muller, C., & Reinecke, H. (2011a). Characterization of high aspect ratio non-conductive ceramic microstructures made by spark erosion. *Microsystem Technologies*, 17 (2), 313-318.
[5] Patel, K. M., Pandey, P. M., & Rao, P. V. (2010). Optimisation of process parameters for multi-performance characteristics in EDM of Al2O3 ceramic composite. *International Journal of Advanced Manufacturing Technology*, 47(9-12), 1137-1147.
[6] Mohri, N., Fukuzawa, Y., Tani, T., Saito, N., & Furutani, K. (1996). Assisting electrode method for machining insulating ceramics. *CIRP Annals-Manufacturing Technology*, 45 (1), 201-204.
[7] Banu, A., Ali, M. Y., & Rahman, M. A. (2014). Micro-electro discharge machining of non-conductive zirconia ceramic: investigation of MRR and recast layer hardness. *International Journal of Advanced Manufacturing Technology*, 75 (1-4), 257-267.
[8] Chen, Y. F., Lin, Y. J., Lin, Y. C., Chen, S. L., & Hsu, L. R. (2010). Optimization of electrodischarge machining parameters on ZrO_2 ceramic using the Taguchi method. *Journal of Engineering Manufacture*, 224 (2), 195-205.
[9] Sabur, A., Moudood, A., Ali, M. Y., & Maleque, M. A. (2013). Investigation of surface roughness in micro-electro discharge machining of nonconductive ZrO_2 for MEMS application. IOP Conference Series: Materials Science and Engineering, 53 (1), 012090.
[10] Schubert, A., Zeidler, H., Wolf, N., & Hackert, M. (2011). Micro electro discharge machining of electrically nonconductive ceramics. *AIP Conference Proceedings*, 1353 (1), 1303-1308.
[11] Schubert, A., Ziedler, H., Kuhn, R, & Hackert-Oschatzchen, M. (2015). Microelectrical discharge machining: a suitable process for machining ceramics. *Journal of Ceramics*, 2015.
[12] Liu, Y. H., Ji, R. J., Li, X. P., Yu, L. L., & Zhang, H. F. (2008). Electric discharge milling of insulating ceramics. Proceedings of the Institution of Mechanical Engineers, Part B: *Journal of Engineering Manufacture*, 222 (2), 361-366.
[13] Izquierdo, B., Sanchez, J. A., Plaza, S., Pombo, I., & Ortega, N. (2009). A numerical model of the EDM process considering the effect of multiple discharges. *International Journal of Machine Tools and Manufacture*, 49 (3), 220-229.
[14] Salonitis, K., Stournaras, A., Stavropoulos, P., & Chryssolouris, G. (2009). Thermal modelling of the material removal rate and surface roughness for die-sinking EDM. *International Journal of Advanced Manufacturing Technology*, 40(3-4), 316-323.
[15] Liu, Y. H., Yu, L. L., Xu, Y. L., Ji, R. J., & Li, Q. Y. (2009). Numerical simulation of single pulse discharge machining insulating Al2O3 ceramic. *Proceedings of the Institution of Mechanical Engineers, Part B: Journal of Engineering Manufacture*, 223 (1), 55-62.
[16] Wong, Y. S., Rahman, M., Lim, H. S., Han, H., & Ravi, N. (2003). Investgation of micro-EDM material removal characteristics using single RC-pulse discharges. *Journal of Materials Processing Technology*, 140 (1), 303-307.
[17] Zahiruddin, M. & Kunieda, M. (2012). Comparison of energy and removal efficencies between micro and macro EDM. *CIRP Annals-Manufacturing Technology*, 61 (1), 187-190.
[18] Kiran, M. P. K. & Joshi, S. S. (2007). Modeling of surface roughness and the role of debris in micro-EDM. *Journal of Manufacturing Science and Engineering*, 129 (2), 265-273.

[19] Alexander, C. K., Sadiku, M. N., & Sadiku, M. (2007). *Fundamentals of Electric Circuits:* McGraw-Hill Higher Education.
[20] Liao, Y. S., Chang, T. Y., & Chuang, T. J. (2008). An on-line monitoring system for a micro electrical discharge machining (micro-EDM) process. *Journal of Micromechanics and Microengineering*, 18 (3), 035009.
[21] Schubert, A., Zeidler, H., Hackert-Oschätzchen, M., Schneider, J., & Hahn, M. (2013). Enhancing micro-EDM using ultrasonic vibration and approaches for machining of nonconducting ceramics. *Journal of Mechanical Engineering*, 59(3), 156-164.
[22] Aligiri, E., Yeo, S. H., & Tan, P. C. (2010). A new tool wear compensation method based on real-time estimation of material removal volume in micro-EDM. *Journal of Materials Processing Technology*, 210(15), 2292-2303.
[23] Dhanik, S., & Joshi, S. S. (2005). Modeling of a single resistance capacitance pulse discharge in micro-electro discharge machining. *Journal of Manufacturing Science and Engineering*, 127 (4), 759-767.
[24] Ji, R., Liu, Y., Zhang, Y., Wang, F., Cai, B., & Fu, X. (2012). Single discharge machining insulating Al2O3 ceramic with high instantaneous pulse energy in kerosene. *Materials and Manufacturing Processes*, 27 (6), 676-682.
[25] Trueman, C. & Huddleston, J. (2000). Material removal by spalling during EDM of ceramics. *Journal of the European Ceramic Society*, 20 (10), 1629-1635.
[26] Abbas, N. M., Solomon, D. G., & Bahari, M. F. (2007). A review on current research trends in electrical discharge machining (EDM). *International Journal of Machine Tools and Manufacture*, 47(7), 1214-1228.